

Instability of viscous flow over a deformable two-layered gel: Experiments and theory

R. Neelamegam, D. Giribabu, and V. Shankar*

Department of Chemical Engineering, Indian Institute of Technology, Kanpur 208016, India

(Received 20 May 2014; published 7 October 2014)

The instability of the flow of a viscous fluid past a soft, two-layered gel is probed using experiments, and the observations are compared with results from a linear stability analysis. The experimental system consists of the rotating top plate of a rheometer and its stationary bottom plate on which the two-layer gel is placed. When the flow between the top plate and the two-layer gel is viscometric (i.e., laminar), the viscosity obtained from the rheometer is a measure of the material property of the fluid. However, after a critical shear stress, there is a sudden increase in apparent viscosity, indicating that the flow has undergone an instability due to the deformable nature of the two-layer gel. Experiments are carried out to quantify how the critical value of fluid shear stress required to destabilize the flow varies as a function of ratio of solid to fluid layer thickness, and the ratio of the shear moduli of the two gels. A linear stability analysis is carried out for plane Couette flow of a Newtonian fluid past the two-layered gel, by assuming the two solid layers to be elastic neo-Hookean materials. In order to compare the experimental and theoretical results, the effective shear modulus (G_{eff} , defined by $H/G_{\text{eff}} = H_1/G_1 + H_2/G_2$) of the two-layer gel is found to be useful, where $H = H_1 + H_2$. Here, H_i and G_i ($i = 1, 2$), respectively, denote the thickness and shear modulus of each layer. Results for the nondimensional parameter $\Gamma_{\text{eff}} = \eta V / (d G_{\text{eff}})$ (V is the velocity of the top plate; η is fluid viscosity, d is the fluid thickness) as a function of solid to fluid thickness H/d obtained from the stability analysis agree well with experimental observations, without any fitting parameters. In general, we find that the flow is more unstable if the softer gel is adjacent to the fluid flow compared to the case when it is not. This suggests that the instability is more interfacial in nature and is crucially dependent on the relative placement of the two layers, and not just on the effective modulus of the two-layer gel. We further show that the theoretical and experimental data for two-layer gels can be suitably collapsed onto the results obtained for a single-gel layer.

DOI: [10.1103/PhysRevE.90.043004](https://doi.org/10.1103/PhysRevE.90.043004)

PACS number(s): 47.20.Ma, 47.61.-k

I. INTRODUCTION

Flow of viscous liquids past soft and deformable solid surfaces is encountered in many biological systems [1,2], as well as in microfluidic devices, where elastomers are the materials of choice in soft fabrication of micron-scale fluid processing units [3,4]. An important issue in such flows is to clearly identify conditions under which the flow remains laminar, and when the flow becomes unstable and undergoes a transition to a more complex flow state. A novel feature in these systems is that the deformable nature of the solid wall by itself can induce new flow instabilities which are absent in flow through rigid channels, and this aspect has been well studied both experimentally [5–10] and theoretically [11–15]. The instability induced by the deformable solid layer in channels of width of $O(100)\mu\text{m}$ could be potentially exploited in promoting mixing [10] in microfluidic devices, by tailoring the shear modulus of the elastomers. However, all prior studies have used a single-layer viscoelastic material to describe the deformation in the soft elastomer. In many biological settings, the deformable wall of the fluid-conveying vessel is multilayered [16,17], and the role of such composite, layered walls on the stability of the flow has not been probed experimentally so far. Even in microfluidic devices, the use of multilayer soft elastomers could potentially enable us to manipulate and control the instability in a better manner. Thus, the study of stability of viscous flow past a layered soft solid is of relevance to both biological and microfluidic

applications. Barring the work of Gkanis and Kumar [18], which reported a theoretical analysis of the stability of plane Couette flow past a wall with depth-dependent shear modulus, this problem has not been addressed in the literature. In this work, we carry out experiments to analyze the effect of a two-layer gel on the stability of the viscous flow between two parallel plates. The experimental observations are compared with predictions from a linear stability calculation performed using the neo-Hookean model for the solid materials. In the remainder of this Introduction, we briefly review relevant literature in this area and motivate the context for the present work.

In fluid flow past deformable solid surfaces, there is a dynamical coupling between the fluid flow and solid deformation, and this “elasto-hydrodynamic” coupling could potentially stabilize or destabilize the flow. Early interest in this subject was mainly motivated by the possibility of using compliant solid coatings to delay transition to turbulence in marine and aerospace applications at high Reynolds number [19–23]. The experiments of Gaster [24] showed that the spatial growth of the instability in a boundary layer is mitigated by the presence of a compliant coating. It is also possible for the deformable wall to destabilize a flow that is otherwise stable in flow past rigid surfaces. This was first suggested in the experiments of Krindel and Silberberg [25] who coated the inner surface of a tube with a gel and found that the pressure drop required for flow in the gel-walled tube is much more than that required for flow in a rigid tube. This observation was linked to the instability of the laminar flow in the tube. Hansen and Hunston [26] conducted experiments on flow over a rotating disk coated with a compliant layer, and showed that

*vshankar@iitk.ac.in

the flow becomes unstable above a critical velocity. Kumaran *et al.* [11] first showed theoretically using a linear elastic model for the solid that the planar Couette flow past a gel slab of finite thickness could become unstable even in the limit of negligible fluid and solid inertia. They suggested that the shear work done by the fluid at the fluid-wall interface is the physical mechanism for energy transfer between mean flow and fluctuations. A similar instability was predicted for flow in a deformable tube by Kumaran [27]. The instability was verified experimentally by Kumaran and Muralikrishnan [5,6] who modified the standard configuration of a commercial rheometer (as explained later in Sec. II) to identify the point of instability in the flow. The flow conditions in these experiments are such that the Reynolds number of the flow is always less than unity. The experimental observations for the critical strain rate at which the instability occurs compared reasonably well with the theoretical predictions of Ref. [11]. Eggert and Kumar [7] carried out experiments to probe the nature of the flow after the instability and found evidence to suggest that the instability is subcritical near its onset. They established this result by observing hysteresis close to the onset of instability. This was in qualitative agreement with the weakly nonlinear stability calculations of Ref. [28]. Gkanis and Kumar [14] argued that for strain rates at which the instability occurs, the base-state deformation is an $O(1)$ quantity, and hence the use of the linearized elasticity model is not strictly correct. They suggested the use of the frame-invariant neo-Hookean model for the solid [29], which led to additional couplings between the base state and fluctuations in the coupled problem. In particular, the first normal stress difference in the base state in the solid gave rise to a short-wave instability, which was absent in the linearized elastic solid model. However, for ratio of solid to fluid thickness of $O(1)$ and higher, the predictions of both the linearized model and the neo-Hookean model are quantitatively similar.

Theoretical studies for the tube geometry were reported in Refs. [12,13,30], and they showed the existence of various types of unstable modes in a deformable tube. Experimental studies [9,10] in gel-walled tubes as well as rectangular channels have now corroborated the theoretical predictions, at least for one type of instability termed the “wall mode” instability. Thus, it can be said that the stability of flow past *single-layer* deformable walls has been understood reasonably well from both experimental and theoretical standpoints. However, in reality, the deformable walls encountered in biological fluid-conveying vessels such as arteries are multilayered [16,17] structures, but could be approximately modeled as a two-layered composite comprising the “media” (the middle layer) and the “adventitia” (the outer layer). Real arteries also exhibit some anisotropy in their mechanical behavior due to the collagen fibers. It is thus of interest to ask how the multilayered structure of the wall affects the instability. Gkanis and Kumar [18] previously carried out linear stability calculations for a linear elastic solid with depth-dependent modulus, as well as for a two-layer linear elastic solid. They concluded that the solid layer which is closer to the liquid layer controls the critical parameters of the instability. One major unresolved issue is whether the multilayer structure of the wall can be described with an effective modulus of the composite layer, or whether the relative placement of the two solid layers

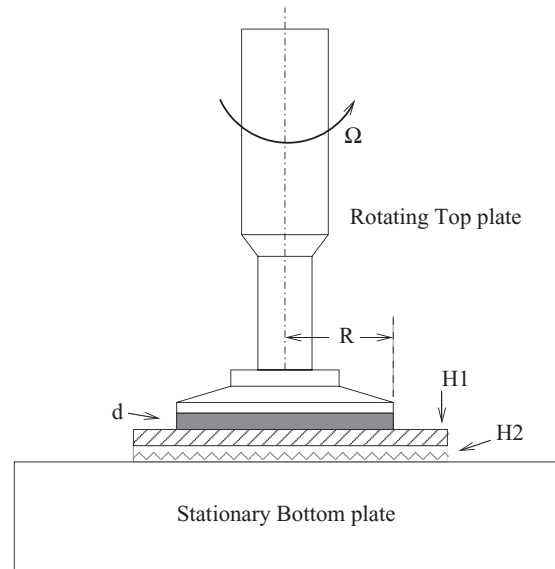


FIG. 1. Schematic diagram of the experimental setup: The standard configuration of the rheometer is modified for studying flow past a soft two-layer gel. The radius of the rotating top plate is R , and the fluid thickness between the rotating top plate and the two-layer gel is d . The gel (of total thickness H) consisting of two layers (bottom layer thickness H_2 and top layer thickness H_1) is placed over the stationary bottom plate of the rheometer.

with respect to the liquid is important. Or, equivalently, is the instability “interfacial” in nature, or is it governed by the effective shear modulus of the material? We address this question in detail below using both experiments and theory. We also demonstrate below how the theoretical result for the instability of flow past a *single-layer* gel could be effectively used to predict the instability of flow past a two-layer gel, by suitably rescaling the results for the two-layer.

The rest of this paper is organized as follows: Sec. II describes the experimental setup and methodology, along with a summary of the characterization of the fluids and soft solids used in the flow experiments. Section III briefly outlines the mathematical formulation of the linear stability calculation for plane Couette flow past a two-layer gel. The results for flow past single- and two-layer gels are discussed in Sec. IV and are compared with theoretical predictions. Here we also show how the data for various two-layer gel configurations can be collapsed onto the results for flow past a *single* gel layer. Finally, Sec. V provides the salient conclusions of the present study.

II. EXPERIMENTAL METHODS AND PROCEDURE

We use the Discovery HR-3 hybrid rheometer (TA Instruments, USA) for studying the instability in flow past the gel, and the MCR 502 (Anton-Paar) rheometer for characterization of the gels. The standard configuration of the Discovery HR-3 rheometer is modified for probing the instability, and the schematic is shown in Fig. 1. The rheometer consists of a stationary bottom plate and rotating top plate. The top plate can be moved vertically to achieve the required gap between the plates, and the normal force measuring arrangement is used

TABLE I. Ratios of two-layer gel thickness (H) to fluid thickness (d) used in the experiments. The error bar on the measured thickness ratio (H/d) is about 3% of the reported value.

Fluid thickness (d) (mm)	Solid thickness (H) (mm)	Thickness ratio (H/d)
1.1	4	3.63
0.5	2	4
0.9	4	4.44
0.7	4	5.7
0.3	2	6.66
0.5	4	8
0.5	6	12
0.3	4	13.33
0.3	6	20

for zero gap adjustment. A soft two-layer gel is placed on the bottom plate, and in order to make the surface of the gel as the zero position, the following procedure is used. The default value of the normal force in the rheometer for detecting the contact is 4.33 N, and use of this high normal force could potentially damage the soft gels used in this study. Hence, instead of using the soft gel surface to set the zero gap, we use glass slides of the same thickness for this purpose. First, we place the soft gel on the bottom plate of the rheometer, and the top plate of the rheometer is brought down until it measures the normal force of 0.2 N. This is now used to determine the thickness of the soft gel. The harder dummy with identical thickness is prepared (using glass microslides) and is next placed on the bottom plate. The surface of the dummy is then used to set the zero position using the default normal force (4.33 N). By this method the error bar in fluid thickness measurement is about 3%. The top plate is raised, and the fluid is now placed on the gel surface (using a dropper) without air entrapment as ensured by visual observation. The top plate is gently lowered to obtain the required fluid thickness, and the excess fluid beyond the edge of the plate is carefully removed using a dropper. To measure the fluid viscosity, the fluid thickness (d) for flow is maintained at 0.3 mm. For flow past two-layer gels, the fluid thickness is varied from 0.3 to 1.1 mm, as summarized in Table I. The radius of the top plate R is 20 mm. The two-layer gel consists of slabs of polyacrylamide or polydimethylsiloxane gels of equal thickness molded one above the other. The interface between the two layers is not chemically cross-linked, but there is strong physical adhesion between the two gel layers, which ensures that the two layers do not slip past each other. The two-layer gel is prepared for different combinations of modulus ratio $G_r = G_2/G_1$ (ratio of bottom to top layer modulus), as summarized in Table II.

The rheometer is operated in a stress-controlled mode, and the angular velocity (rad/s) at the outer rim of the top plate is measured. The stress is increased as linear function of time (stress ramp) at the rate of 4 Pa/s from 1 to 3000 Pa, and the strain rate and apparent viscosity were recorded by the rheometer [5]. The stress is computed as $\tau = 2M/\pi R^3$, where M is the applied torque and the shear rate is computed as $\dot{\gamma} = \Omega R/d$. When the flow is viscometric, the shear rate is related to the shear stress as $\tau = \eta\dot{\gamma}$. This relation is strictly

TABLE II. The ratio of bottom to top layer shear moduli $G_r = G_2/G_1$ and the individual moduli of the bottom and top gel layers used in the experiments.

G_r	Top layer modulus	Bottom layer modulus
	G_1 (kPa)	G_2 (kPa)
0.14	6.38 ± 0.11	0.90 ± 0.10
0.21	4.21 ± 0.31	0.90 ± 0.10
0.34	6.38 ± 0.11	2.17 ± 0.07
0.41	4.05 ± 0.10	1.67 ± 0.03
2.42	1.67 ± 0.03	4.05 ± 0.10
2.94	2.17 ± 0.07	6.38 ± 0.11
4.68	0.90 ± 0.10	4.21 ± 0.31
7.08	0.90 ± 0.10	6.38 ± 0.11

valid for viscometric flow of a Newtonian fluid. The apparent viscosity increases sharply when the flow is not viscometric, and the corresponding shear rate is taken as the critical shear rate at which the viscometric flow becomes unstable. We also carried out limited steady-flow experiments at a given value of shear stress, and the results for the critical shear rate for instability obtained from both steady flow and stress ramp modes are found to be the same. To characterize the rheological properties of the gel, we use the oscillatory-shear mode. In all our experiments, the temperature of the fluid is allowed to settle to the ambient temperature (25 °C).

A. Fluid preparation

The parallel plate geometry ($R = 20$ mm) is used for characterizing the fluids in our flow experiments. Three different Newtonian fluids are used in these experiments in order to investigate the effects of variation in fluid properties on the flow instability: (a) silicone oil (Lobachemie) with viscosity 0.33 Pa s at 25 °C, (b) silicone oil (Dow Corning, 200 fluid) with viscosity 1 Pa s, and (c) 60 wt/wt % polyethylene oxide solution (PEO, Lobachemie, $M_w \sim 6000$ gmol⁻¹) in deionized water is prepared as follows: 12 g of PEO and 8 g of deionized (DI) water are taken in a beaker and mixed thoroughly using a magnetic stirrer for 12 h at 30 °C. Polyethylene oxide is a flexible polymer and its radius of gyration $R_g = 3.1$ nm. The viscosity of the 60% PEO solution is nearly independent of shear rate for the range of shear rates used in our study (up to 3380 s⁻¹; see Fig. 2). Hence, the PEO solution can be treated as a Newtonian fluid for the present purposes. The viscosities of the various fluids used in this study are summarized in Table III. The fluids used are impermeable

TABLE III. Viscosities of different fluids used in the experiments. The viscosities were measured at 25 °C using the parallel plate geometry, and the error bar in the measurements is within 5% of the reported values.

Fluid	Viscosity (Pa s)
Silicone oil (Lobachemie)	0.33
Silicone oil (Dow Corning)	1.00
60 wt/wt% PEO mixed in DI water	0.44

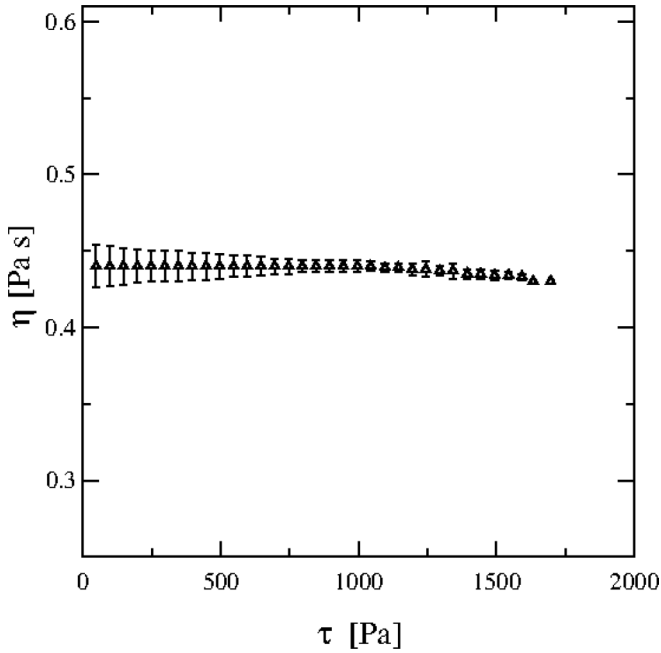


FIG. 2. Viscosity of the PEO solution as a function of shear stress. Data demonstrate that the fluid shows negligible shear thinning and remains Newtonian in the range of stresses probed in this study. Measurement was carried out at 25°C using the parallel plate geometry.

and nonreactive with the respective gels on which flow studies are conducted.

B. Soft two-layer gel preparation and characterization

We use both polyacrylamide and polydimethylsiloxane (PDMS) gels in this study. First, we discuss the preparation and fabrication of polyacrylamide gels. The stock solutions of acrylamide (Himedia), bisacrylamide (Lobachemie), and ammonium per sulphate (Qualigens) were prepared with 20, 0.5, and 1.25 weight percentage, respectively, using DI water. The tetramethyl ethylenediamine (Himedia) stock is prepared by mixing 0.625 ml of the original solution with 93.75 ml DI water. The final solution is prepared by mixing DI water and the above stock solutions in exact proportion to achieve the required monomer (acrylamide) concentration of 5–8%. The gel is prepared using the following steps (schematically depicted in Fig. 3).

(a) The microscopic glass slides (1 mm thickness) with dimensions 1.25 cm × 7.6 cm are pasted on the sides of a glass plate (side 10 cm × 10 cm), and the arrangement forms a square-shaped trough. The “spacer” is prepared by pasting glass slides (thickness 1 mm, side 0.5 cm × 0.5 cm) in the four corners of the trough (see Fig. 3). (b) The gel consists of two layers in which the bottom layer is prepared by dispensing the acrylamide solution in the trough until it spreads out uniformly to the height of the spacers. (c) A 6.75 cm × 6.75 cm glass plate (3 mm thickness) is placed on the spacers, and the solution was allowed to cross-link for 2 h. (d) After the bottom gel layer is formed, the glass plate is carefully removed without disturbing the gel layer, which now has a smooth top surface. (e) Then the other acrylamide solution

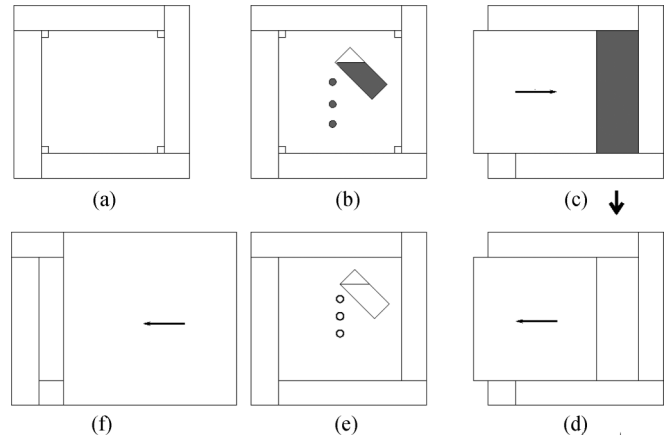


FIG. 3. Preparation of the two-layer gel. (a) The microscopic glass slides are pasted on the sides of a glass plate, and this template forms a well. Small square-shaped glass slides were pasted on the four corners of the well to ensure that the thickness of the bottom layer of the two-layer gel is uniform. (b) The constituents of the polymer gel are dispensed in the above template. (c) A glass plate is placed on the small square-shaped glass slides, and we allowed 2 h for the solution to get cross-linked. (d, e) The glass plate is carefully removed and the constituents of the polyacrylamide gel are added. (f) A larger glass plate is kept on the template, and the constituents are allowed to cross-link.

(with different monomer concentration) is dispensed on the bottom layer until the trough is filled. (f) The glass plate (side 10 cm × 10 cm) is placed on side walls of the trough without air entrapment, and the mixture is allowed to cross-link for 2 h. The glass plate is removed, and the whole arrangement is placed on the rheometer for the experiment to be carried out. A similar method is employed for making single-layer gels.

We next discuss the preparation and fabrication of two-layer gels made using PDMS. The PDMS gel is prepared by mixing Dow Corning Sylgard 184 (viscosity 3.7 Pa s) base and Sylgard 184 curing agent in the required ratio. Polymerization of the mixture consisting of Sylgard 184 base and curing agent gives rise to harder PDMS gels. In order to reduce the shear modulus, we mix silicone oil (Dow Corning 200; measured viscosity is 1 Pa s and density is 0.97 g/cc) at different proportions to bring down the shear modulus. We prepared the PDMS gel by mixing Sylgard 184 base to the curing agent and silicone oil in the proportion 1:0.154:6.54. This corresponds to 85% silicone oil in the total mixture (see Table V). The gel mixture of

TABLE IV. Rheological properties (G' and G'') of polyacrylamide gels prepared with different monomer concentrations at 25°C. The reported G' and G'' is averaged over the frequency range 0.1–10 Hz.

Monomer concentration wt/wt%	G' (kPa)	G'' (kPa)
5	0.90 ± 0.10	0.02 ± 0.02
6	2.17 ± 0.07	0.02 ± 0.02
7	4.21 ± 0.31	0.05 ± 0.07
8	6.38 ± 0.11	0.02 ± 0.02

TABLE V. Rheological properties (G' and G'') of polydimethylsiloxane (PDMS) gels prepared with different % of silicone oil mixed with the Sylgard base at 25 °C. The reported G' and G'' averaged over the frequency range 0.1–10 Hz.

% silicone oil in PDMS base	G' (kPa)	G'' (kPa)
85	4.05 ± 0.10	0.26 ± 0.23
87.5	1.67 ± 0.03	0.19 ± 0.18

Sylgard and silicone oil results in much softer PDMS gel after curing. The proportion of silicone oil present in the gel mixture is further increased to obtain more softer gels. For softer gels, the proportion of Sylgard 184 base to curing agent to silicone oil (viscosity 1 Pa s) used is 1:0.19:8.33. This corresponds to 87% silicone oil in the total mixture (see Table V). Two-layer gels of PDMS with different shear moduli are prepared in a manner similar to polyacrylamide two-layer gels described above. The main difference is that the curing of PDMS gels is carried out in a oven at 70 °C for 12 h.

The linear viscoelastic characteristics of the gel is determined using the parallel plate (diameter 2.5 cm) geometry of the Anton-Parr (MCR502) rheometer in following manner. The gel slab (single layer) is placed on the bottom plate, and the top plate is brought in contact with the gel surface till the normal force reaches 0.2 N. An oscillatory stress (of magnitude 10 Pa) is applied to the top plate, and its angular displacement is measured in the frequency range from 0.1 to 10 Hz. The gel thickness used in these experiments is 4 mm, and the measurements are made at 25 °C. The results are summarized in Tables IV and V. Figure 4 shows the linear viscoelastic properties of various single-layer polyacrylamide gels (prepared using different monomer concentrations) as a

function of frequency. The storage moduli of the gels show a constant plateau region in the frequency range 0.1–10 Hz [5], and the plateau value increases with monomer concentration. Gels with monomer concentration 5–8% are prepared in order to benchmark our measurements with reported [5,6] storage modulus values. We found that the handling of very soft gels prepared with less than monomer concentration 5% becomes difficult.

The observed viscoelastic properties of polyacrylamide gels prepared with different monomer concentrations were compared with the earlier reported results [5,6]. The reported shear modulus for different monomer concentrations 5%, 6%, and 7% are 950, 2300, and 3600 Pa, respectively, and the observed values are 900, 2200, and 4200 Pa, suggesting good agreement between the present characterization and previous work. The loss modulus data are plotted in terms of gel viscosity $\mu_g = G''/\omega$ in Fig. 4(b). Figure 5 shows the results for PDMS gels, whose shear moduli are comparatively low (in the order of 1000 Pa), and the gels are nonsticky.

III. THEORY

In this section we briefly outline the theoretical formulation to predict the stability characteristics of plane Couette flow past a two-layer gel. The earlier analysis of Gkanis and Kumar [14] for a single neo-Hookean solid layer is generalized for a neo-Hookean two-layer configuration here. Although the experiments are carried out in the rotating-disk geometry, it is nonetheless useful to carry out the theoretical analysis for the planar case. This is because the ratio of the outer radius of the top plate to fluid thickness is very large, and locally the streamlines are not strongly curved near the edges of the flow. Since the linear velocity is maximum near the rim of the two disks, the instability is expected to originate close to

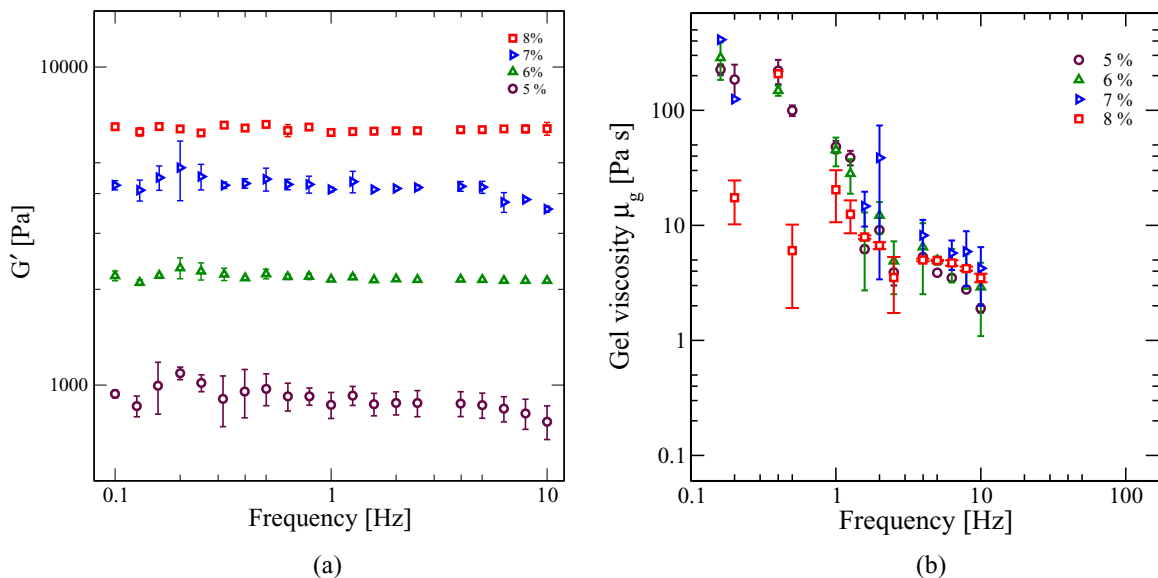


FIG. 4. (Color online) Characterization of the polyacrylamide gels. (a) Storage modulus (G') of polyacrylamide gel as function of frequency. G' is approximately constant for the frequency range for different monomer concentrations: 5% (open circle), 6% (open triangular up), 7% (open triangular right), and 8% (open square), and the plateau value increases with increasing monomer concentration. (b) Gel viscosity $\mu_g = G''/\omega$ as a function of frequency. The experiments are carried out using 2.5 cm diameter parallel plate geometry of Anton Paar rheometer (MCR502) at 25 °C. The gel thickness is 4 mm.

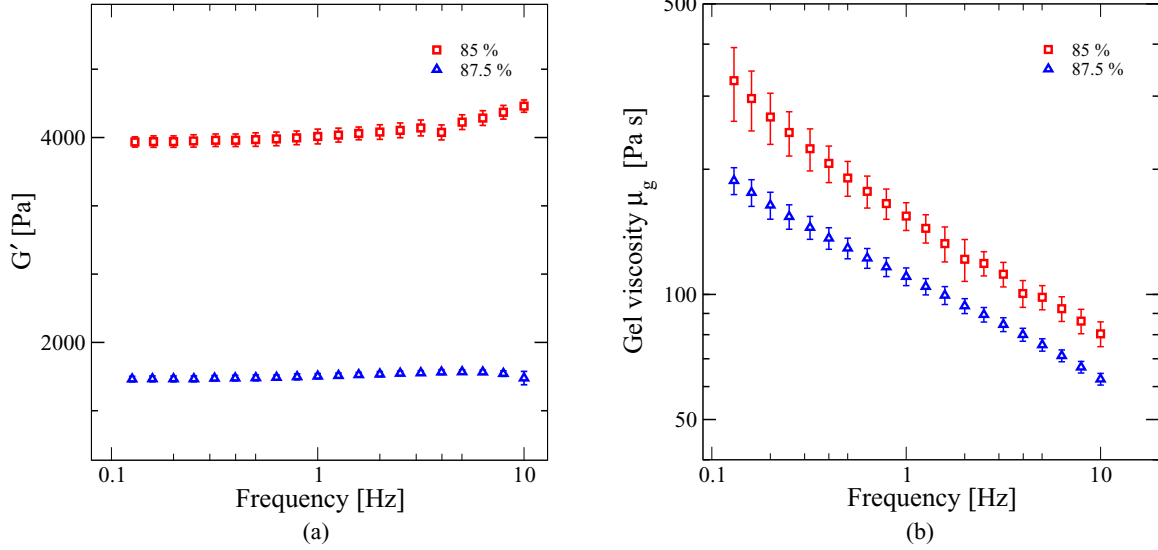


FIG. 5. (Color online) Characterization of the PDMS gels. (a) Storage modulus (G') of PDMS gel as function of frequency. Two different concentrations of the silicone oil (viscosity 1 Pa s) concentration in the gel mixture is used here, *viz.*, 85% (open square) and 87.5% (open triangular). The G' is nearly constant for the frequency range. (b) Gel viscosity as a function of frequency. The experiments are carried out using 2.5 cm diameter parallel plate geometry of Anton Paar rheometer (MCR502) at 25°C. The gel thickness is 4 mm.

the rim, and the parallel flow approximation is reasonable in that region. The system (Fig. 6) consists of two solid layers having different shear moduli G_1 and G_2 and thicknesses H_1 and H_2 , respectively. This composite solid layer is assumed to be perfectly bonded to the bottom plate. In the unperturbed state, fluid of thickness d undergoes planar Couette flow on the top of the two-layer gel and is confined by the top rigid plate, which moves with a velocity V at $z = d$. In the absence of inertia, the governing equations for the fluid and solid layers are given below. The fluid is governed by mass and momentum conservation equations:

$$\nabla \cdot \mathbf{v} = 0, \quad \nabla \cdot \boldsymbol{\tau} = 0, \quad (1)$$

where \mathbf{v} is velocity and $\boldsymbol{\tau}$ is total stress in fluid. The total stress is given by

$$\boldsymbol{\tau} = -p_f \mathbf{I} + \mu[\nabla \mathbf{v} + (\nabla \mathbf{v})^T]. \quad (2)$$

Here p_f is the pressure in the fluid, \mathbf{I} is the identity tensor, and μ is the viscosity of the fluid. The deformable solids in the two-layer gel are modeled as purely elastic, incompressible, neo-Hookean materials. In the Lagrangian description (following Gkanis and Kumar [14]), the deformation in the solid is

described by

$$\mathbf{x}(\mathbf{X}, t) = \mathbf{X} + \mathbf{u}(\mathbf{X}, t), \quad (3)$$

where \mathbf{X} is reference position at $t = 0$, \mathbf{x} is the current position of particle at any time t , and \mathbf{u} is (Lagrangian) displacement of the particle.

The equations of mass and momentum conservation in the two solids are given by

$$\det(\mathbf{F}_i) = \det\left(\frac{\partial \mathbf{x}_i}{\partial \mathbf{X}}\right) = 1, \quad (4)$$

$$\nabla_X \cdot \mathbf{P}_i = 0, \quad \mathbf{P}_i = \mathbf{F}_i^{-1} \cdot \boldsymbol{\sigma}_i, \quad (5)$$

where $i = 1, 2$, for top and bottom layers, respectively, \mathbf{F}_i is the deformation gradient tensor, \mathbf{P}_i is the Piola-Kirchhoff stress tensor, and $\boldsymbol{\sigma}_i$ is Cauchy stress in solid of the form

$$\boldsymbol{\sigma}_i = -p_{si} \mathbf{I} + G_i \mathbf{F}_i \cdot \mathbf{F}_i^T. \quad (6)$$

The governing equations of fluid and solids are nondimensionalized by scaling velocities with $\frac{G_1 d}{\eta_f}$, distances with d , time with $\frac{\eta_f}{G_1}$, pressure and stresses with G_1 (top layer shear modulus).

A. Linear stability theory

In linear stability analysis, small perturbations in the form of Fourier modes are imposed on velocity, pressure, and displacement fields. If f' represents the perturbation to any dynamical variable f , then

$$f'(x, z, t) = \tilde{f}(z) \exp(ikx + st). \quad (7)$$

In this study, we restrict the perturbations to be two-dimensional, as have most studies in this area. Further, we consider temporal stability, and hence k is a real quantity, while s is complex. If $\text{Re}[s] > 0$, the flow is temporally unstable. After introducing infinitesimal perturbations to the base state,

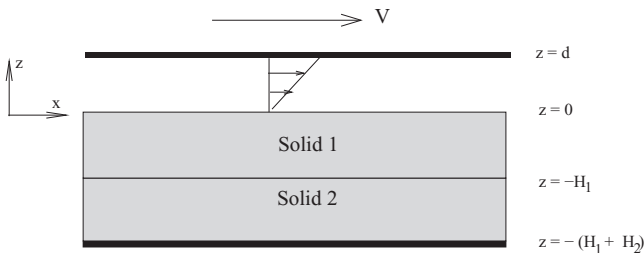


FIG. 6. Schematic representation and coordinate system used in the theoretical analysis of plane Couette flow past a deformable two-layer gel.

the linearized governing equations of fluid and solid are given by (with $D \equiv d/dz$) the following:

Fluid:

$$D\tilde{v}_z + ik\tilde{v}_x = 0, \quad (8)$$

$$-ik\tilde{p}_f + (D^2 - k^2)\tilde{v}_x = 0, \quad (9)$$

$$-D\tilde{p}_f + (D^2 - k^2)\tilde{v}_z = 0, \quad (10)$$

Solid 1:

$$D\tilde{x}_{13} + ik\tilde{x}_{11} - i\Gamma_{\text{top}}k\tilde{x}_{13} = 0, \quad (11)$$

$$-ik\tilde{p}_{s1} + (D^2 - k^2)\tilde{x}_{11} = 0, \quad (12)$$

$$i\Gamma_{\text{top}}k\tilde{p}_{s1} - D\tilde{p}_{s1} + (D^2 - k^2)\tilde{x}_{13} = 0, \quad (13)$$

Solid 2:

$$D\tilde{x}_{23} + ik\tilde{x}_{21} - ik\frac{\Gamma_{\text{top}}}{G_r}\tilde{x}_{23} = 0, \quad (14)$$

$$-ik\tilde{p}_{s2} + G_r(D^2 - k^2)\tilde{x}_{21} = 0, \quad (15)$$

$$ik\frac{\Gamma_{\text{top}}}{G_r}\tilde{p}_{s2} - D\tilde{p}_{s2} + G_r(D^2 - k^2)\tilde{x}_{23} = 0, \quad (16)$$

where $G_r = \frac{G_2}{G_1}$ is the ratio of bottom to top layer shear moduli in the two-layer gel, and $\Gamma_{\text{top}} = V\eta/(G_{\text{top}}d)$ is the nondimensional strain rate in the fluid based on the top layer shear modulus.

The above linearized governing equations are supplemented by boundary conditions at the fluid-solid interface, solid-solid interface, and the rigid walls. At the rigid walls, the fluid velocities (at $z = d$) and the solid displacements [at $z = -(H_1 + H_2)$] become zero. The velocity and stress continuity conditions at the fluid-solid interface are similar to the ones given in Ref. [14], which are obtained after linearizing about the unperturbed flat interface. At the solid-solid interface, we assume continuity of velocity and stresses. Upon linearizing, the velocity and stress continuity conditions at the unperturbed fluid-solid and solid-solid interfaces of the two-layer configuration are the following:

$$\tilde{v}_x + \Gamma_{\text{top}}\tilde{x}_{13} - \alpha\tilde{x}_{11} = 0, \quad (17)$$

$$\tilde{v}_z - \alpha\tilde{x}_{13} = 0, \quad (18)$$

$$D\tilde{x}_{11} + [\Gamma_{\text{top}}D + ik(1 - \Gamma_{\text{top}}^2)]\tilde{x}_{13} - D\tilde{v}_x - ik\tilde{v}_z = 0, \quad (19)$$

$$\tilde{p}_{s1} - 2D\tilde{x}_{13} - \tilde{p}_f + 2D\tilde{v}_z - k^2\gamma\tilde{x}_{13} = 0, \quad (20)$$

$$\tilde{x}_{11} = \tilde{x}_{21}, \quad \tilde{x}_{13} = \tilde{x}_{23}, \quad (21)$$

$$D\tilde{x}_{11} + [ik(1 - \Gamma_{\text{top}}^2)]\tilde{x}_{13} - \frac{1}{G_r}\{[-ik(G^2 - G_r^2)]\tilde{x}_{23} + G_r^2 D\tilde{x}_{21}\} = 0, \quad (22)$$

$$-\tilde{p}_{s1} + 2D\tilde{x}_{13} + \tilde{p}_{s2} - 2G_r D\tilde{x}_{23} = 0. \quad (23)$$

This completes the specification of the eigenvalue problem for the growth rate s , which is obtained as follows. The linearized differential equations in the fluid and the two solids are solved to obtain velocity and displacement fields, and the solutions will have undetermined constants. These solutions are substituted in the boundary and interface conditions, and

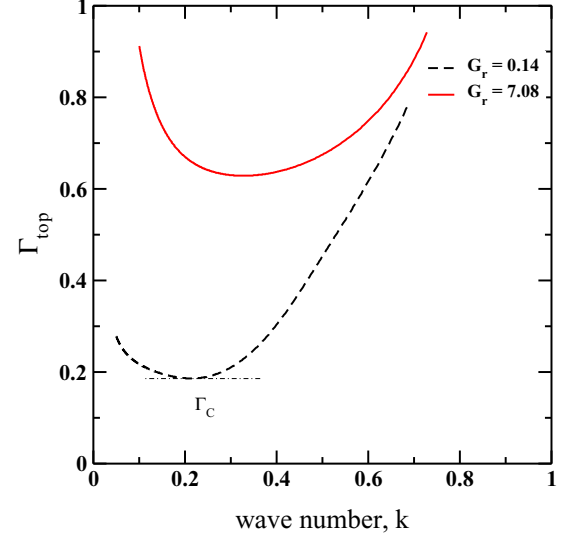


FIG. 7. (Color online) The variation of Γ_{top} vs k for specified values of $H_1/d = H_2/d = 4$, and $G_r = 0.14$ (hard-on-top) and $G_r = 7.08$ (soft-on-top), the flipped configuration. The minimum of this curve is the critical nondimensional strain rate Γ_c at which the flow becomes unstable.

for nontrivial solutions, the determinant of the resultant matrix is set to zero, which will yield the characteristic equation for the growth rate s . For the system considered here, the characteristic equation is a second order equation in s , which is solved using the symbolic package Mathematica. The result from the theoretical calculation is the neutral stability curve for Γ (required for instability) as a function of wave number k , for specified values of G_r , H_1 , and H_2 . A representative neutral curve from our calculations is shown in Fig. 7. The minimum value of this curve is the critical value Γ_c required to destabilize the flow. It is this critical value (for specified values of H_1 , H_2 , and G_r) that is compared with the critical strain rate observed in experiments.

IV. RESULTS

A. Flow over single-layer gels

Before proceeding to characterize the viscous flow past two-layer gels, we first briefly describe the results for flow over a single-layer gel in this subsection. We initially characterized the fluid flow between the rigid plates of the rheometer. For this purpose, we used silicone oil of viscosity 1 Pa s, and the fluid thickness is 0.3 mm. The shear stress was increased at a constant rate of 4 Pa/s up to a maximum of 3000 Pa. The observed apparent viscosity is constant with shear stress, indicating that the flow between rigid plates is viscometric in nature. The maximum Reynolds number reached in all of our experiments is about 1. The same protocol is used for the other two fluids, *viz.*, silicone oil with viscosity 0.33 Pa s and the PEO solution. Both these fluids also exhibited Newtonian behaviour when the stress is increased up to 3000 Pa. When a single gel layer is placed on the bottom plate of the rheometer, the apparent viscosity for flow over the gel is close to the viscosity observed for flow between the rigid plates until the flow remains viscometric and laminar. When

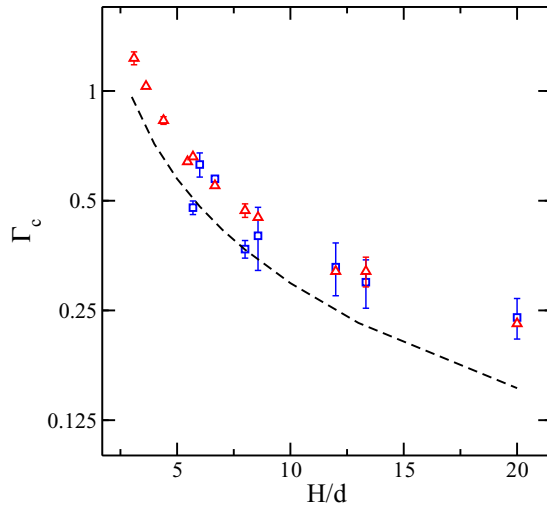


FIG. 8. (Color online) Viscous instability for flow past single polyacrylamide gel layers: The dimensionless critical strain rate for instability Γ_c as a function of H/d . Silicone oils with different viscosities [1 Pa s (open triangular), 0.33 Pa s (open square)] are used to carry out the experiments. The various polyacrylamide gels used in the experiments have shear moduli 0.9, 2.17, 4.21, and 6.38 kPa. For each of these shear moduli, gels of different thicknesses (H/d) were prepared. The dashed line is the theoretically predicted Γ_c for various H/d using a neo-Hookean model. The experiments are carried out using a 4 mm diameter parallel plate (DHR3 rheometer) at room temperature.

the flow becomes unstable, an abrupt increase in viscosity is observed, and the stress at which the viscosity increases is identified as the critical shear stress. Beyond the critical stress, the flow does not possess the concentric flow stream lines (assumed in viscometric flows), and the increase in viscosity is not therefore a true reflection of the intrinsic fluid property. Instead, it is a manifestation of the altered, nonviscometric flow in the rheometer [5,6]. The transition happens because of the coupling between the fluid flow and deformation in the solid [11,14]. When the stress was increased beyond the critical value, the surface of the gel gets damaged. However, if we stop the experiment before the gel damage and repeat the experiment again, the critical shear stress for instability is reproducible. Until the point of instability, the shear stress in the fluid is the product of viscosity and the strain rate in the fluid. Thus, the critical nondimensional parameter $\Gamma_c = \dot{\gamma}_c \eta / G'$ that is used in theoretical predictions can be obtained from the experiments as τ / G' , where τ is the critical shear stress at which there is an abrupt increase in the viscosity.

Figure 8 shows the variation of the parameter Γ_c with the ratio of soft solid layer to fluid thickness H/d for flow of silicone oil over polyacrylamide gels. The polyacrylamide gels used in this study have shear moduli in the range 900 to 6200 Pa. The fluid thickness (d) used in our experiments is 0.3, 0.5, 0.7, 0.9, and 1.1 mm. The gel thickness (H) used in our experiments is 2, 4, and 6 mm.

The experimental results were benchmarked with earlier experimental results [5] by using silicone oil of different grades (viscosity 0.33 and 1 Pa s), as well as with theoretical predictions from the linear stability analysis. The experiments

are carried out for a range of H/d values, and the observed critical strain rate Γ_c decreases monotonically with H/d . This variation is in good agreement with the theoretical predictions from the linear stability analysis of viscous flow past a neo-Hookean solid [14]. The highest value of fluid thickness that can be held between the disks (by surface tension) is 1.5 mm. Further, the lowest values of gel thickness that could be fabricated is about 2 mm. Thus, we were not able to probe further low values of the ratio of solid to fluid thickness $H/d < 1$. The linear stability analysis of viscous flow on neo-Hookean solid [14] also predicts a short-wave instability when the dimensionless thickness $H/d < 1$. Our experimental range of H/d is such that this short-wave instability is not the most critical mode, and the finite wave-number instability predicted in Ref. [11] is the most critical mode. The dashed line is the theoretically predicted value of Γ_c for various H/d using the neo-Hookean model. The experimental and theoretical values are reproduced to benchmark (Fig. 8) our results with results reported in Refs. [5,6] and [14]. Earlier experiments [5,6] used silicone oil with 1 Pa s viscosity; however, the current experiments are carried out with both 0.33 and 1 Pa s viscosity silicone oils. The results show good agreement (between the two solutions used in the experiments, and with theoretical predictions) even when we use silicone oil with different viscosity. These results thus show that the instability is independent of fluid viscosity, when plotted in terms of Γ_c . Here we use a neo-Hookean solid model [14] for linear stability analysis because it accommodates the finite deformation in a solid (in its base state). In contrast, earlier studies used a linear elastic solid model for linear stability analysis [11].

We next discuss the results obtained from experiments using PEO solution flow over a PDMS gel, in order to establish that the instability is generic in flow past soft gel surfaces and is independent of the specific fluid-solid combination used to study the flow. The critical strain rate Γ_c as a function of H/d for viscous flow on PDMS gel is shown in Fig. 9.

The dashed line shows the theoretical predictions for viscous flow past neo-Hookean solid, and this agrees reasonably well with the experimentally observed results without any fitting parameters. The theoretical prediction underpredicts the Γ_c value required to destabilize the flow, and this discrepancy could be because of compressibility effects in the gel.

Thus, the experimental results from two different fluid-gel combinations agree quite well within error bars, and the experimental observations are also in reasonably good agreement with the theoretical predictions. We now proceed to discuss the experimental results for flow past a soft two-layer gel.

B. Flow over two-layer gels

The main motivation to carry out flow experiments over two-layer gels is to explore whether the instability in this configuration would be determined by the “effective” shear modulus of the two-layer gel, or by the relative placement of the soft and hard gels next to the fluid. The effective shear modulus is calculated from the relation $H/G_{\text{eff}} = H_1/G_1 + H_2/G_2$, where H , H_1 , H_2 are the total, top, and bottom layer thicknesses, respectively, and G_1 , G_2 are shear moduli of the top and bottom layers, respectively. This effective

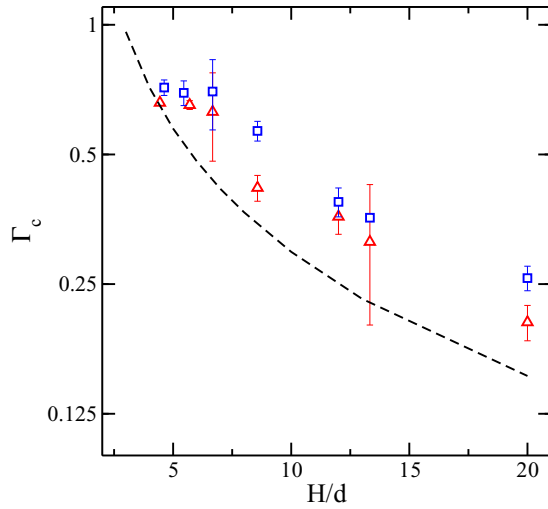


FIG. 9. (Color online) Viscous instability in the flow of PEO solutions past single-layer PDMS gels: The critical nondimensional strain rate Γ_c as a function of H/d . The dashed line is the theoretical prediction (using neo-Hookean model) of Γ_c for different values of H/d . The shear modulus of the PDMS gel used is 4.05 kPa (open triangular) and 1.67 (open square) kPa. The experiments are carried out using a 4 mm diameter parallel plate (DHR3 rheometer) at room temperature.

modulus G_{eff} is calculated by assuming that the two layers undergo an affine deformation under shear, and that at the interface between the two solid layers there is continuity of displacement and stress. We have directly measured the effective modulus of the two-layer gel using the rheometer and have verified that this observed value agrees well with the value obtained by substituting the individual gel moduli

(measured experimentally) in the expression for the effective modulus. This agreement confirms the validity of displacement and stress continuity at the interface between the gels. For two-layer gels with equal thickness, G_{eff} remains the same regardless of the relative placement of the two layers. To this end, we prepare gels comprising of two layers of equal thickness but with different shear moduli. We then carry out experiments by first placing the softer (of the two-layer) gel adjacent to the fluid, followed by another set of experiments where the harder (of the two-layer) gel is adjacent to the fluid. In order to present and compare the experimental results for both the configurations (i.e., harder layer on top and softer layer on top), we use the effective shear modulus of the two-layer gel G_{eff} (defined above) to define a modified nondimensional parameter $\Gamma_{\text{eff}} = V\eta/dG_{\text{eff}}$. For the two-layer gel, the nondimensional strain rate could also be defined as $\Gamma_{\text{top}} = V\eta/dG_{\text{top}}$ (based on the shear modulus of the top layer) or using $\Gamma_{\text{bottom}} = V\eta/dG_{\text{bottom}}$ (based on the shear modulus of the lower layer). The earlier theoretical study by Gkanis and Kumar [18] has shown that the flow instability is more influenced by the shear modulus of the material close to the fluid. Thus, in principle, the nondimensional parameters that determine the stability of the flow past the two-layer gel are Γ_{eff} , H/d , H_1/H_2 , η_{r1} , η_{r2} , and $G_r = G_2/G_1$. In our experiments we deal exclusively with gel layers of equal thickness $H_1 = H_2$, so $H_1/H_2 = 1$. In our theory, we have assumed the gel layers to be purely elastic, and hence $\eta_{r1} = \eta_{r2} = 0$. Usually dissipation in the gel provides a stabilizing effect, and hence the theoretical predictions will underestimate the critical shear rate for instability. A wide range of ratio of the shear moduli G_r of the two gel layers are used in our experiments, as summarized in Table II.

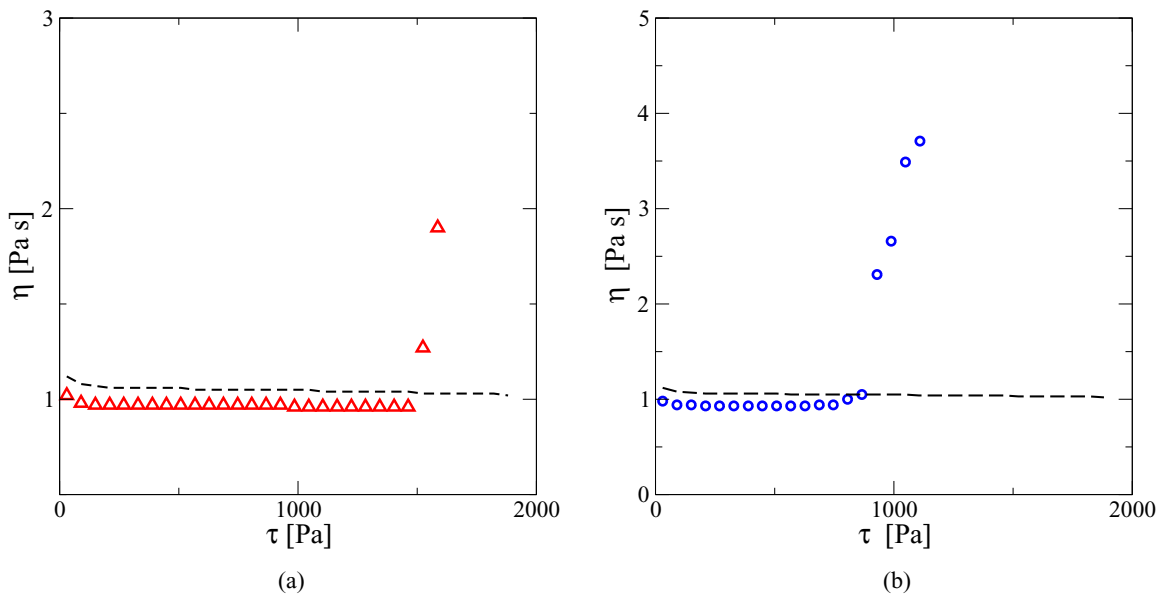


FIG. 10. (Color online) Onset of instability in the viscous flow past a two-layer gel as indicated by the apparent viscosity from the rheometer: The fluid used in the experiments is silicone oil with viscosity is 1 Pa s. The two-layer configuration consists of two gels with shear moduli $G' = 6375$ Pa and 900 Pa. (a) Results when the hard layer is on top (open triangles) with $G_r = 0.41$; (b) results when the soft layer is on top (open circles), $G_r = 7.08$. The dashed line denotes results from flow between rigid plates without the gel. The fluid and two-layer gel thicknesses used in the experiments are 0.3 and 2 mm, respectively. The experiment is carried out at 25 °C. The parallel plate geometry of DHR3 rheometer is used in the experiment, and the top plate diameter is 40 mm. The shear stress is increased at the rate of 4 Pa/s.

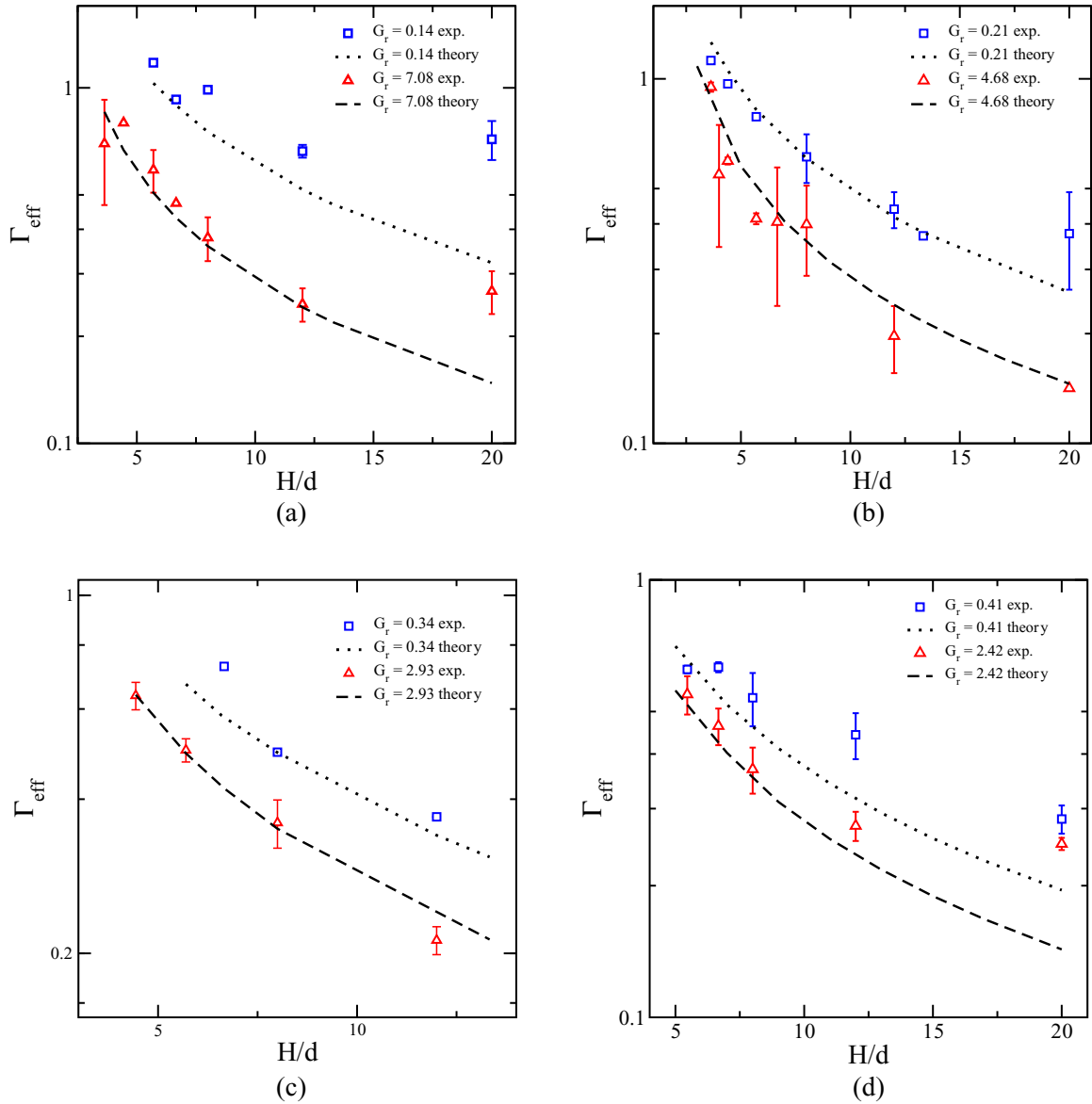


FIG. 11. (Color online) Instability of viscous flow past various two-layer gels: Γ_{eff} as a function of H/d for different values of G_r indicated in each panel at the upper right corner. (a)–(c) Results for flow of silicone oil over polyacrylamide two-layer gels; (d) results for flow of PEO solution over PDMS two-layer gels. Each panel shows the two configurations, *viz.*, when the soft gel is on top and when hard gel is on top. Open squares represent data when the harder gel is on top, and the corresponding theoretical prediction is indicated by dotted lines. Open triangles represent the for the case where the gels are flipped (*i.e.*, softer gel on top), and the dashed line represents the corresponding theoretical predictions. Two types of silicone oils (with viscosity 0.33 and 1 Pa s) are used as the fluid for each configuration in panels (a)–(c). The theoretical predictions are obtained using the neo-Hookean model for the gels.

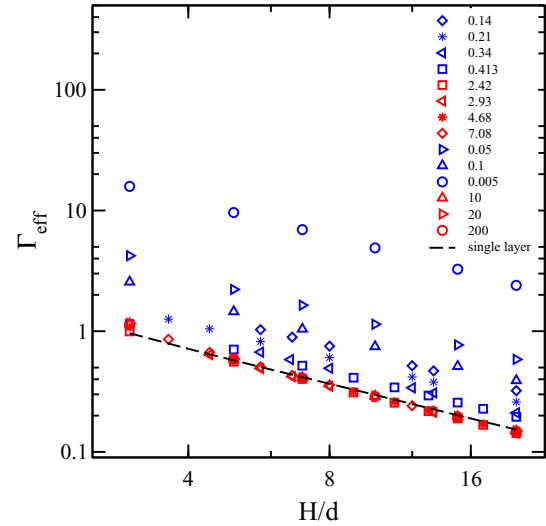
In Fig. 10 we show the measured viscosity from the rheometer (in the stress-controlled mode) for the case of fluid flow past the two-layer gel placed on the bottom plate of the rheometer. For lower values of shear stresses in the fluid, the viscosity from the rheometer agrees with the reported viscosity of the fluid in between two rigid plates. However, after a critical shear stress, the apparent viscosity increases sharply. This is a signature of the instability induced in the system due to the deformability of the two-layer gel. The value of the shear stress at which the apparent viscosity increases is taken as the critical shear stress, and the critical shear rate ($\dot{\gamma}_c$) is calculated by dividing the critical shear stress by the viscosity of the fluid. This critical shear rate is nondimensionalized in the form of the

parameter $\Gamma_{\text{eff}} = \dot{\gamma}_c \eta / G_{\text{eff}}$. In Fig. 11 we plot the critical strain rate (Γ_{eff}) as a function of H/d for different values of G_r . In Fig. 11(a), the two-layer gel (polyacrylamide layers with $G_r = 7.08$) consists of a soft layer on top of the hard layer, and the observed nondimensional critical strain rate (Γ_{eff}) is very close to the result predicted from linear stability analysis for viscous flow past the neo-Hookean two-layer gel. However, if we have a harder layer on top of a softer layer ($G_r = 0.14$; configuration of the two-layer gel flipped), the observed critical strain rate (Γ_{eff}) value is much larger compared to the case when the soft layer was on top ($G_r = 7.08$). For both cases, the critical strain rate decreases monotonically with H/d and agrees well with theoretical predictions.

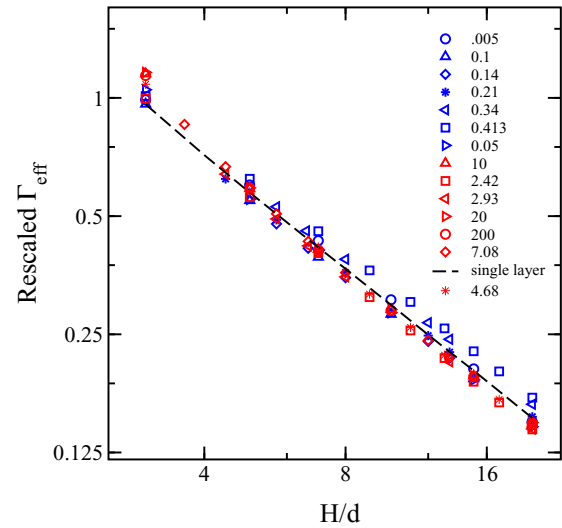
Figures 11(b) and 11(c), show the critical strain rate Γ_{eff} as a function of H/d , respectively, for $G_r = 4.68$ and 2.93 and the corresponding flipped configuration with $G_r = 0.21$ and 0.34 for flow over the polyacrylamide two-layer gel. For the two-layer gel with soft layer on top ($G_r = 4.68$ and 2.93), the experimental observations show good agreement with theoretical predictions. When the hard layer is on top, the critical Γ_{eff} increases with a decrease in G_r . Thus, when the hard layer is on top, the instability can be delayed further by changing the G_r value. Figure 11(d) shows Γ_{eff} as a function of H/d for viscous flow (of PEO solution) over the polydimethylsiloxane two-layer gel. These results are obtained for a different fluid-gel system in order to demonstrate the generality of flow instability. The nondimensional critical strain rate for two-layer gel with hard on top ($G_r = 0.41$) and soft on top ($G_r = 2.42$) shows good agreement with theoretical predictions obtained using neo-Hookean model.

Figure 12(a) shows the Γ_{eff} as a function of H/d obtained from theory for different G_r . The experiments are carried out for $G_r = 0.14, 0.2, 0.34, 0.41, 2.42, 2.93, 4.68,$ and 7.08 . The theoretical predictions were computed for a more wider range of G_r values in order to understand how the gel characteristics affect the flow instability. In Fig. 12(a) we observe that the results for Γ_{eff} vs H/d (for various $G_r > 1$), when the soft layer is on top, lie very close to the single-layer result, for $H/d > 2$. This trend can be explained as follows. For the purposes of this discussion, we define the nondimensional total solid thickness $H^* = H/d$, and the nondimensional individual layer thicknesses $H_{\text{top}}^* = H_1/d$ and $H_{\text{bottom}}^* = H_2/d$. When the softer layer is on the top ($G_r > 1$), as we increase G_r from unity to very large values, eventually we approach the limit of a softer layer with shear modulus G_{top} and thickness $H^*/2$, since the harder bottom layer now behaves like a rigid solid in this limit of $G_r \rightarrow \infty$. If we use $\Gamma_{\text{top}} = V\eta/(G_{\text{top}}d)$ to define the nondimensional strain rate, for $G_r = 1$, Γ_{top} will take the value corresponding to a single layer of thickness H^* , and for $G_r \rightarrow \infty$, Γ_{top} will approach the value corresponding to a single layer of thickness $H^*/2$ (since the bottom half layer approaches the rigid limit). For $H^* > 1$, earlier studies [11] have shown that $\Gamma_{\text{top}} \propto 1/H^*$. Thus, the Γ_{top} value will increase from the value for a single layer of thickness H^* (when $G_r = 1$) to twice this value when $G_r \rightarrow \infty$. From the definition of G_{eff} , $H^*/G_{\text{eff}} = H_{\text{top}}^*/G_{\text{top}} + H_{\text{bottom}}^*/G_{\text{bottom}}$, which when $H_1 = H_2$ becomes $G_{\text{eff}} = 2G_{\text{top}}/(1 + G_r^{-1})$. For $G_r \rightarrow \infty$, $G_{\text{eff}} \rightarrow 2G_{\text{top}}$. The relation between Γ_{eff} and Γ_{top} is given by $\Gamma_{\text{eff}} = \Gamma_{\text{top}}(1 + G_r^{-1})/2$, which for $G_r \rightarrow \infty$ becomes $\Gamma_{\text{eff}} = \Gamma_{\text{top}}|_{G_r \gg 1}/2$. We had just argued above that $\Gamma_{\text{top}}|_{G_r \gg 1}$ will take twice its value for a single layer when $G_r \rightarrow \infty$, which implies that in this limit $\Gamma_{\text{eff}} = \Gamma_{\text{top}}|_{G_r=1}$. Thus, Γ_{eff} will remain essentially constant as G_r is varied from unity to very large values, and this constant is the same as the critical Γ for a single layer of thickness H . Thus, when the softer layer is on top, this explains the reason why curves for different G_r collapse onto the curve for a single gel layer of thickness H , when the results are plotted in terms of Γ_{eff} .

However, the results for the hard-on-top two-layer configuration show that the Γ_{eff} vs H/d curve shifts upwards with decrease in G_r . This can be explained as follows. When $G_r = 1$, the results for the two-layer gel would again



(a) Results from theory



(b) Results collapsed onto a master curve

FIG. 12. (Color online) Collapse of theoretical results for flow past two-layer gels with different G_r values. (a) Theoretically predicted Γ_{eff} as a function of H/d for different G_r . The dashed line indicates the theoretically predicted Γ as a function of H/d for a single solid layer. (b) The data of panel (a) collapse on to the single-layer results, if the results for two-layer gels with the hard layer on top are rescaled as $1.5\Gamma_{\text{eff}}G_r^{0.6}$. The results for two-layer gels with the soft layer on top lie close to the single-layer curve *without* rescaling.

correspond to those for a single layer of thickness H . As G_r is decreased further, the layer below becomes progressively softer, and in the limit $G_r \ll 1$, we would reach the limit of a hard layer which is exposed to zero shear stress condition at the solid-solid interface. Earlier studies [28] have shown that in this limit (termed the “adsorbed gel” limit), the critical Γ_{top} decreases compared to the case when the gel is rigidly bonded to rigid surface. Our numerical results show that for $G_r \ll 1$, $\Gamma_{\text{top}} \propto G_r^{0.4}$. This implies that $\Gamma_{\text{eff}} = \Gamma_{\text{top}}(1 + G_r^{-1})/2$ in the

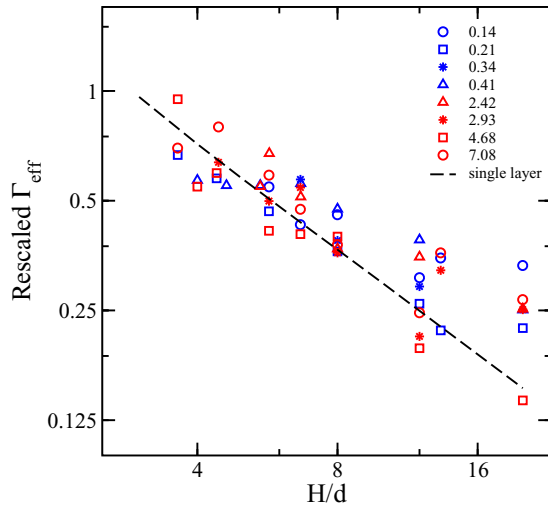


FIG. 13. (Color online) Collapse of experimental results (symbols) for Γ_{eff} for two-layer gels with different G_r values onto the theoretical curve (dashed line) for a single solid layer. The results for two-layer gels with the harder gel on top were rescaled using $1.5\Gamma_{\text{eff}}G_r^{0.6}$.

limit of $G_r \ll 1$ will become $\Gamma_{\text{eff}} \propto G_r^{-0.6}$. Thus, if we multiply the results for different values of $G_r < 1$ by $G_r^{0.6}$, then the results will collapse onto a single curve. Figure 12(b) shows the superposed Γ_{eff} vs H/d , where the hard-on-top results are multiplied by $1.5\Gamma_{\text{eff}}G_r^{0.6}$. The results for the case when the softer layer is on top are left unscaled, since they already collapse onto the results for a single layer, for reasons given above. After the data rescaling and collapse, we find that the results for the rescaled Γ_{eff} for both configurations (soft-on-top and hard-on-top) now lie close to the single-layer results for Γ_c . We further note that the rescaled Γ_{eff} scales as $\Gamma_{\text{eff}} \propto 1/H^*$ for $H^* > 1$, as found in the case of single gel layer [11]. This demonstrates that the single-layer results could be used to predict the trends of instability of viscous flow past the two-layer gel. In a similar fashion, the experimentally observed hard-on-top two-layer gel results are superposed using the rescaling procedure explained above. Figure 13 shows good agreement even for rescaled experimental observations for two-layer gels with the single layer results. The superposed experimental and theoretical results [Figs. 12(b) and 13] show that Γ_{eff} decreases with H/d for different G_r (when $H_1 = H_2$).

In their theoretical analysis, Gkanis and Kumar [18] used a simpler linear elastic model for their two-layer gel, but they reported results only for $H_2 \neq H_1$ thus precluding a direct comparison of our results with their results.

V. CONCLUSIONS

We have carried out both experiments and linear stability analysis to understand the stability of viscous flow of Newtonian liquids past deformable, two-layer gels. The experiments were carried out for a range of shear moduli ratio G_r and for different fluid-gel combinations. The critical nondimensional strain rate Γ_{eff} is lower when the softer layer is adjacent to the fluid, when compared to the case when the harder layer is next to the fluid. The experimental results show that the instability is “interfacial” in nature in that it is crucially dependent on whether the softer layer is adjacent to the liquid or not. Thus, to predict the instability accurately, it is not sufficient to model the two-layer configuration as a single layer with an effective modulus. The results of the experiments were compared with predictions from a linear stability calculation, and we find good agreement without any fitting parameters. We further showed that when the results are plotted in terms of $\Gamma_{\text{eff}} = V\eta/G_{\text{eff}}d$, where G_{eff} is the effective shear modulus of the two-layer gel, it is possible to collapse the results for both the configurations (hard-on-top, $G_r < 1$ and soft-on-top, $G_r > 1$) onto a single master curve which lies close to the results for the stability of flow past a single gel layer. Thus, we have shown that the stability characteristics of flow past a two-layer gel can be readily predicted from the results obtained for flow over a single-layer gel. The results of our study also suggest that the instability past soft deformable solids can be manipulated and controlled using a two-layer gel instead of single layers. For example, in microfluidic devices, by tailoring the composition of the two-layer gel, the onset instability can be delayed or advanced depending on whether laminar flow is desirable or not. Our observations and predictions could also be relevant to biological flows, where arteries are typically multilayered, and our results suggest that if the innermost layer is softer, then it is easier to destabilize these flows.

ACKNOWLEDGMENT

Mr. Puneet Aggarwal is acknowledged for his assistance in carrying out the preliminary experiments.

- [1] J. B. Grotberg and O. E. Jensen, *Ann. Rev. Fluid Mech.* **36**, 121 (2004).
- [2] J. B. Grotberg, *Phys. Fluids* **23**, 021301 (2011).
- [3] J. C. McDonald and G. M. Whitesides, *Acc. Chem. Res.* **35**, 491 (2002).
- [4] T. M. Squires and S. R. Quake, *Rev. Mod. Phys.* **77**, 977 (2005).
- [5] V. Kumaran and R. Muralikrishnan, *Phys. Rev. Lett.* **84**, 3310 (2000).
- [6] R. Muralikrishnan and V. Kumaran, *Phys. Fluids* **14**, 775 (2002).
- [7] M. D. Eggert and S. Kumar, *J. Colloid Interface Sci.* **278**, 234 (2004).
- [8] A. Shrivastava, E. L. Cussler, and S. Kumar, *Chem. Eng. Sci.* **63**, 4302 (2008).
- [9] M. K. S. Verma and V. Kumaran, *J. Fluid Mech.* **705**, 322 (2012).
- [10] M. K. S. Verma and V. Kumaran, *J. Fluid Mech.* **727**, 407 (2013).
- [11] V. Kumaran, G. H. Fredrickson, and P. Pincus, *J. Phys. II* **4**, 893 (1994).
- [12] V. Shankar and V. Kumaran, *J. Fluid Mech.* **395**, 211 (1999).
- [13] V. Shankar and V. Kumaran, *J. Fluid Mech.* **408**, 291 (2000).
- [14] V. Gkanis and S. Kumar, *Phys. Fluids* **15**, 2864 (2003).
- [15] V. Gkanis and S. Kumar, *J. Fluid Mech.* **524**, 357 (2005).

- [16] R. P. Vito and S. P. Dixon, *Annu. Rev. Biomed. Eng.* **5**, 413 (2003).
- [17] G. A. Holzapfel, T. C. Gasser, and R. W. Ogden, *J. Elasticity* **61**, 1 (2000).
- [18] V. Gkanis and S. Kumar, *Phys. Rev. E* **73**, 026307 (2006).
- [19] T. B. Benjamin, *J. Fluid Mech.* **9**, 513 (1960).
- [20] M. T. Landahl, *J. Fluid Mech.* **13**, 609 (1962).
- [21] P. W. Carpenter and A. D. Garrad, *J. Fluid Mech.* **155**, 465 (1985).
- [22] P. W. Carpenter and A. D. Garrad, *J. Fluid Mech.* **170**, 199 (1986).
- [23] M. Gad-el-Hak, in *IUTAM Symposium on Flow Past Highly Compliant Boundaries and in Collapsible Tubes*, edited by P. W. Carpenter and T. J. Pedley (Kluwer Academic, Amsterdam, 2003), pp. 191–229.
- [24] M. Gaster, in *Turbulence Management and Relaminarisation*, edited by H. W. Liepmann and R. Narasimha (Springer-Verlag, Berlin, 1988), pp. 285–304.
- [25] P. Krindel and A. Silberberg, *J. Colloid Interface Sci.* **71**, 34 (1979).
- [26] R. J. Hansen and D. L. Hunston, *J. Fluid Mech.* **133**, 161 (1983).
- [27] V. Kumaran, *J. Fluid Mech.* **294**, 259 (1995).
- [28] V. Shankar and V. Kumaran, *J. Fluid Mech.* **434**, 337 (2001).
- [29] G. A. Holzapfel, *Nonlinear Solid Mechanics* (John Wiley and Sons, Chichester, 2000).
- [30] V. Shankar and V. Kumaran, *Eur. Phys. J. B* **19**, 607 (2001).